

ELASTIC ELECTRON SCATTERING AT LARGE MOMENTUM TRANSFER*

R. G. Arnold[†]
 The American University
 Washington D.C. 20016

and

Stanford Linear Accelerator Center
 Stanford University, Stanford, California 94305

ABSTRACT

A review is given of elastic electron scattering at large momentum transfer ($Q^2 > 20 \text{ fm}^{-2}$) from nuclei with $A \leq 4$. Recent experimental results are reviewed and the current problems in our interpretation of these results are pointed out. Some questions for future experiments are posed, and a preview of possible future measurements is presented.

INTRODUCTION

The electromagnetic form factors of nucleons and nuclei measured in electron scattering experiments form some of the basic data from which we derive much of our knowledge of nucleon and nuclear structure. The form factors of the lightest nuclei ($A \leq 4$) are particularly important because they serve as the touch stones against which we can compare our most precise microscopic theories. Measurements at large momentum transfer probe these systems with increased resolution and are expected to be sensitive to such details as high momentum parts of nuclear wave functions, relativistic kinematics, the effects of meson exchange currents, and eventually to the internal structure of the nucleons. The experiments discussed in this review have been performed or proposed in the period of the last four years by the American University Group [1] at SLAC.

RECENT PROGRESS - THE DEUTERON

In our first experiment [2] on elastic ed scattering, incident electrons with energies from 5 to 19 GeV were sent through a 30 cm long liquid deuterium target, and elastically scattered electrons were measured at a scattering angle of 8° in coincidence with the recoil nuclei using two large spectrometers. Elastic cross sections were measured in the momentum transfer range 0.8 to 6 GeV^2 (20 to 160 fm^{-2}). The coincident detection method was crucial to the success of the measurement and produced nearly background free data down to cross sections of $10^{-38} \text{ cm}^2/\text{sr}$. The cross section for elastic scattering is given by

$$\frac{d\sigma}{d\Omega} = \sigma_{\text{mott}} [A(Q^2) + B(Q^2) \tan^2(\theta/2)] \quad (1)$$

Scattering at 8° measures the $A(Q^2)$ function.

* Work supported by the Department of Energy under contract number DE-AC03-76SF00515.

† Supported by the National Science Foundation under Grant Numbers GP-16565, MPS75-07325, PHY75-15986.

In the past, the two main goals of elastic ed scattering have been to differentiate between deuteron wave function models and to determine the neutron electric form factor G_{En} using the nonrelativistic impulse approximation (NRIA). The nucleon form factors enter $A(Q^2)$ through the square of the isoscalar electric form factor $G_{ES} = G_{Ep} + G_{En}$. The proton electric form factor is measured out to $Q^2 = 3 \text{ GeV}^2$ and is basically of the dipole shape. The neutron G_{En} is unknown above $Q^2 = 1 \text{ GeV}^2$, and below that is very small, perhaps consistent with zero except for the slope at $Q^2 = 0$. The beating of the small G_{En} against the larger and generally better known G_{Ep} in the squared G_{ES} makes $A(Q^2)$ sensitive to small variations in G_{En} .

The deuteron $A(Q^2)$ at large Q^2 is, however, quite complicated, and straightforward tests of models of neutron structure and n-n potentials are not so easy. In addition to the currents due to the nucleons, it is expected that at large Q^2 the meson exchange currents (MEC) and perhaps the isobar currents, caused by mutual excitation of the internal degrees of freedom of the nucleons, should make some contributions to the form factors. At very large Q^2 (how large is very large??) the internal structure (quarks??) of the nucleons may determine the structure functions and a truly "first principles" calculation would start with the quark wave functions. To date there does not exist such a complete calculation, but we do have some advances to report.

There are several approaches, in the language of nuclear physics, to a relativistic impulse approximation (RIA) calculation of the deuteron structure functions.

Two effects must be included: (a) relativistic kinematics, and (b) at least one nucleon must be allowed to be off the mass shell. One method is to start with covariant formulae and then transform away the negative energy states leaving results expressed in terms of corrections to some order in $(Q/m)^2$. F. Gross, in a series of paper [3,4,5], has adopted the alternative approach where he keeps the negative energy states and makes a complete calculation including contributions from the small components of the deuteron wave function (P states).

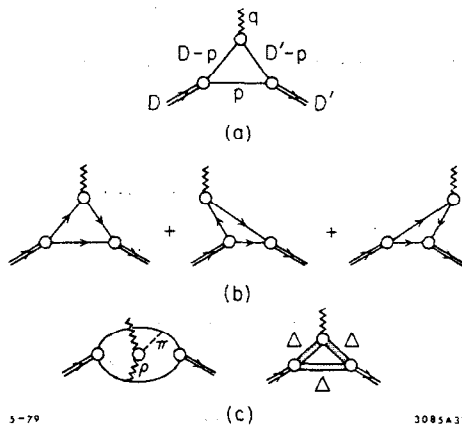


Fig. 1. (a) The relativistic Feynman diagram of the impulse approximation, (b) three nonrelativistic time-ordered diagrams included in the RIA. Backward moving lines are anti-particles. (c) and (d) examples of two processes not included in the RIA. (c) a meson exchange diagram, (d) the isobar contribution.

The RIA calculation [4] begins with the covariant diagram of Fig. 1(a), which includes the three time ordered diagrams of Fig. 1(b) where the interacting nucleon is allowed to be off shell. This approach includes in a natural way to all orders in $(Q/m)^2$ or $(v/c)^2$ both the standard impulse terms and the terms where the photon splits into $n\bar{n}$, which are viewed in

other language as the MEC pair terms. It does not include the genuine MEC currents of Fig. 1(c) or the isobar currents of Fig. 1(d). Four invariants are required to describe the npd vertex, and these can be written so they have the character of wave

functions. Two of these functions are the familiar S and D state wave functions, u and w , present in the non-relativistic treatment, and the two additional wave functions are P states associated with the extra degrees of freedom present when on nucleon is in the virtual Dirac states.

The formulae for the charge, quadrupole, and magnetic structure functions, G_C , G_Q and G_M , are derived in a general way and can be evaluated with any deuteron wave functions. In particular if one chooses to neglect the P states, the formulae give the deuteron structure functions to all orders of $(Q/m)^2$ for any choice of u and w . A complete calculation requires a set of 4-component wave functions. We have evaluated the relativistic formulae numerically [4] using the deuteron models shown in Fig. 2. The 4-component models, indexed by the mixing parameter λ , were obtained by Buck and Gross [5] from solutions to the relativistic wave equation. The P states are numerically small (0.5 to 2 percent of the total wave function), but at large Q^2 they can make

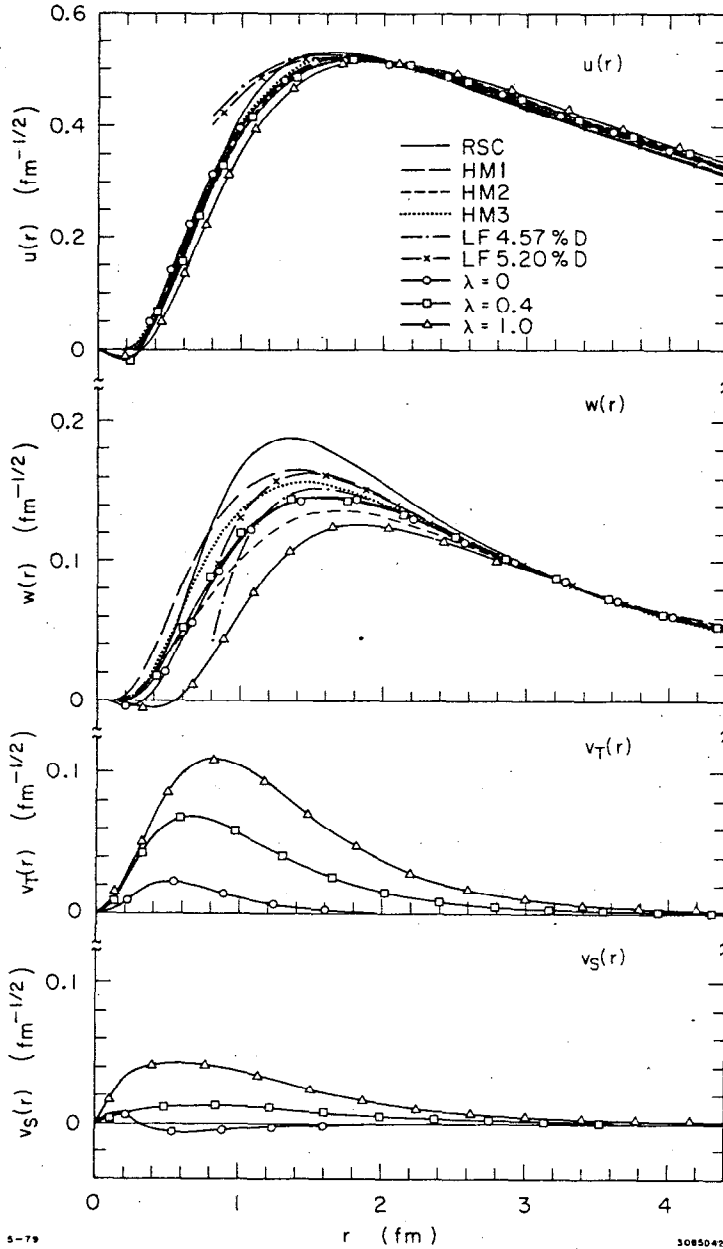


Fig. 2. A collection of deuteron wave functions. (a) the S state, (b) the D state, (c) and (d) the two P states. The 2-component models are: Reid soft core (Ref. [8]), three Holinde-Machleidt models (Ref. [6]), two Loman-Feshbach models with different % D state (Ref. [7]). The 4-component Buck-Gross models (Ref. [5]) are labeled with the mixing parameter λ , which determines the form of the π -n coupling. For $\lambda=0$ the coupling is pure $\gamma_5\gamma_\mu$, for $\lambda=1$ it is pure γ_5 .

appreciable contributions to the structure functions.

To investigate the effects of relativistic kinematics, without the inclusion of the negative energy states, we evaluated the formulae using the 2-component nonrelativistic models in Fig. 2. The results for $A(Q^2)$ are shown in Fig. 3 and in more concise form in Fig. 4 where the ratio of the relativistic to the nonrelativistic results are plotted. The relativistic correction is fairly model independent out to Q^2 of approximately 60 fm^{-2} . The effect on the fundamental form factors G_C , G_Q and G_M is generally to shift the position of diffraction minima to lower Q^2 and increase the height of the following maxima.

Figs. 3 and 4 reveal the basic problem with $A(Q^2)$ in the impulse approximation using dipole form factors. All the models give results which fall below the data by factors of 2 to 10. The overall effect of relativistic kinematics is to depress the nonrelativistic results and further widen the difference between the data and theory.

Results for $A(Q^2)$ using three of the Buck-Gross 4-component models together with the RSC-NR result are presented in Fig. 5. The principle difference between the models in these curves and those of Fig. 3 is the inclusion here of the P states.

An investigation of the effects of the P states indicates that they tend to have the opposite effect of the relativistic kinema-

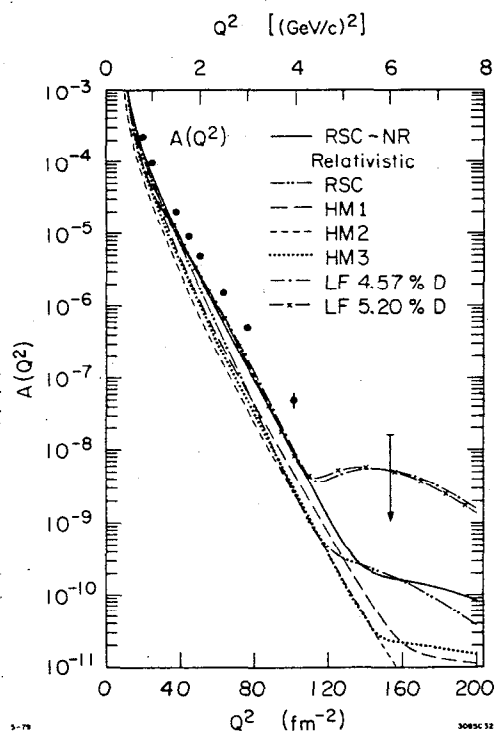


Fig. 3. The deuteron elastic structure function $A(Q^2)$ evaluated in the RIA using the 2-component models in Fig. 2. The curve RSC-NR, determined from the nonrelativistic Reid soft core model, is presented for comparison. Dipole nucleon form factors were used with $G_{En} = 0$.

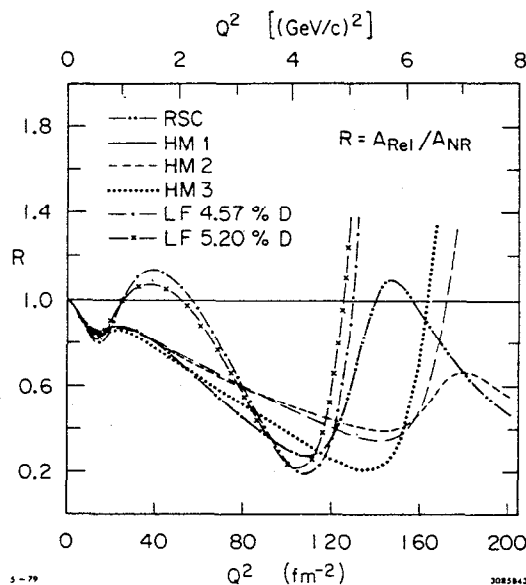


Fig. 4. Relativistic kinematic corrections to the structure function $A(Q^2)$. The ratio of A calculated using the RIA formula to A calculated using the nonrelativistic formulae is given for each 2-component model in Fig. 2.

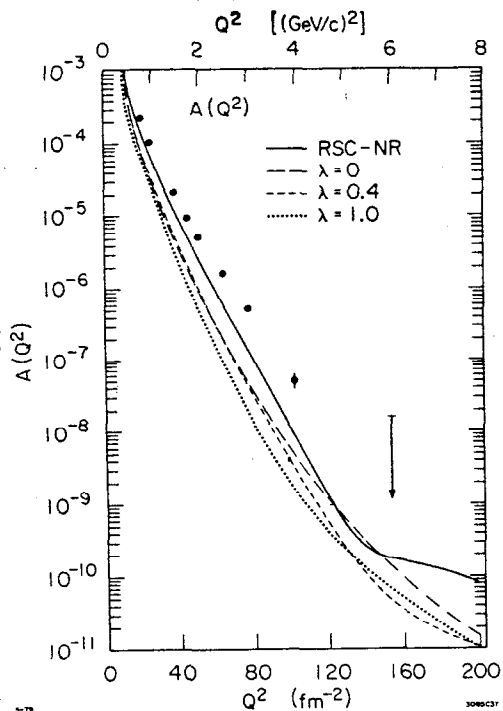


Fig. 5. The deuteron elastic structure function $A(Q^2)$ evaluated in the RIA using three of the 4-component models from Ref. [5]. The RSC-NR curve is the nonrelativistic Reid soft core result. Dipole nucleon form factors were used with $G_{En} = 0$.

the structure functions in that region in addition to those due to the body form factors. As Fig. 6 indicates, the data for $A(Q^2)$ seem to eliminate the possibility of such a dip.

To avoid this problem we assembled a collection of form factors we call "Best Fit". It is not the result of a comprehensive fit but each curve does accurately represent the available data. The G_{En} is taken from the fit by Galster *et al.* [10]. To display the sensitivity of $A(Q^2)$ to variations in G_{En} , we have plotted in Fig. 6 the curves using the "Best Fit" with G_{En} set to zero. The curve labeled Dipole + $F_{1n} = 0$ is an attempt to indicate what possible form G_{En} could take to give agreement with the $A(Q^2)$ data. The assumption

tics, i.e., they shift diffraction minima to higher Q^2 and lower the height of 2nd diffraction maxima. The effect of the P states on the structure functions is model dependent; the curves with different mixing parameter λ differ significantly from each other indicating that the P state contributions are sensitive to the form of the π -n coupling.

We have also investigated various choices for the neutron G_{En} . In Fig. 6 is an example of $A(Q^2)$ for one 4-component model evaluated with 5 different versions of G_{En} displayed in Fig. 7. The results for the dipole form with $G_{En} = 0$ are too low. The IJL parameterization [9] for G_{En} goes through zero and becomes negative above $Q^2 = 38 \text{ fm}^{-2}$ with absolute value comparable to G_{Ep} .

Therefore, G_{ES} goes through a sharp minimum

at about 85 fm^{-2} ,

which introduces a sharp dip in

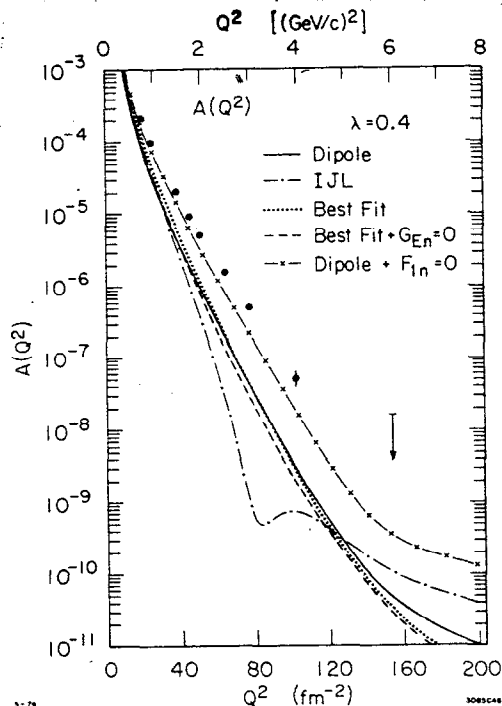


Fig. 6. The deuteron $A(Q^2)$ evaluated in the RIA using the 4-component model with $\lambda = 0.4$ and five versions of the neutron structure function G_{En} presented in Fig. 7.

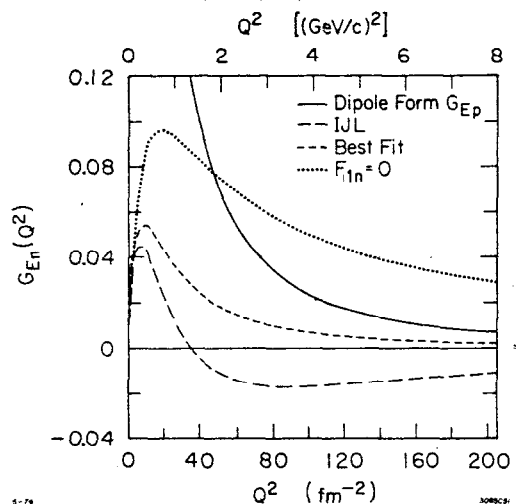


Fig. 7. Various estimates for the neutron structure function G_{En} . The curves are: Best Fit from Galster *et al.* (Ref. [10]); IJL from Ref. [9]; and $F_{1n}=0$ leading to the form given in Eq. (2). For comparison the dipole curve for G_{Ep} is also shown.

of Gari and Hyuga [26] for example, that the genuine isoscalar MEC may also make big contributions to $A(Q^2)$ at large Q^2 , and a straightforward deduction of G_{En} from this calculation is not possible.

To summarize, the deuteron $A(Q^2)$ at large Q^2 presents a rather complicated problem. The overall size of the featureless curve depends in a complex way on many factors. The individual form factors G_C , G_Q and G_M have sharp diffraction features that are very sensitive to the details of the models, but unfortunately, this sharp structure is completely obscured in the total $A(Q^2)$. What is required is a comprehensive relativistic treatment taking into account all the important currents. It would also be helpful for someone to compare in detail the contributions from the so-called MEC pair terms with the alternative treatment in the 4-component RIA. Hopefully the present confusion over the definition of exchange currents can be cleared up.

RECENT PROGRESS - HELIUM

We recently measured electron scattering from ^3He and ^4He at large Q^2 at SLAC [11]. Prior to this experiment there existed something of a crisis in the 3-body problem. Using any of the respectable n-n potentials in Faddeev or variational 3-body calculations does not give good agreement with the ^3He charge form factor. The theoretical minima are at too large Q^2 and the height of the second maxima are too small by factors of 3 to 4. This situation is somewhat improved by the addition of the MEC corrections [15], but still the disagreement persists and is regarded as a serious problem.

that the Dirac form factor F_{1n} is equal to zero is consistent with the prediction of the symmetric quark model for the nucleon structure where the valence quarks are all in a spacially symmetric ground state, and gives, with $\tau = Q^2/4M_n^2$:

$$G_{En} = \tau G_{Mn} = -\mu_n \tau G_{Ep} \quad (2)$$

This parameterization gives a value for G_{En} about a factor of two higher than the Best Fit value, and is at the upper edge of the large experimental [10] error bars in the Q^2 range up to 1 GeV^2 .

From Fig. 6 we conclude that it is possible, assuming for the moment that genuine MEC contributions can be ignored, to get fairly good agreement with the data for $A(Q^2)$ using reasonable values for G_{En} . However we also are aware, from the work

Our measurement was performed in a manner similar to that for the deuteron with elastically scattered electrons detected at 8° in coincidence with the recoil nuclei. The target in this case was gaseous helium at 10 and 50 atm. When scattering at 8° , the cross section is given mostly by the function $A(Q^2)$, which in terms of the charge F_{ch} and magnetic F_{mag} form factors is:

$$A(Q^2) = \left[F_{ch}^2 + \mu^2 \tau F_{mag}^2 \right] / (1 + \tau) \quad (3)$$

The present situation is summarized in Fig. 8. The Faddeev calculations give F_{ch} a factor of 4 to 10 below the data from $Q^2 = 0.8$ to 2 GeV^2 . These theories predict a 2nd diffraction minimum around $Q^2 = 2 \text{ GeV}^2$ but it is not possible to state clearly that such a feature is visible in the new data.

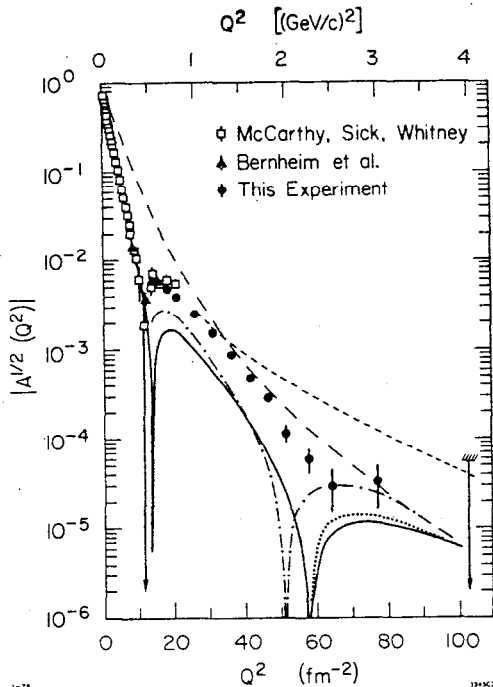


Fig. 8. ^3He elastic structure function data at large Q^2 from Ref. [11], together with previous data (Ref. [12]), and theoretical predictions for F_{ch} and A^2 . The curves are: solid, F_{ch} Faddeev (Ref. [13]); dotted, F_{ch} Faddeev (Ref. [14]); dot-dashed, Faddeev (Ref. [13]) plus MEC (Ref. [15]); small-dashed, A^2 DSQM (Ref. [16]); large-dashed, A^2 RIA (Ref. [17]).

stand how the parts of the wave function with larger angular momentum could contribute more to the charge density at larger radius. This observation may be an important clue to the source of the problem.

One difficulty with the interpretation of Fig. 8 is that the theoretical contributions for F_{mag} at large Q^2 were not available at the time that figure was prepared, and F_{mag} is not measured beyond $Q^2 = 0.8 \text{ GeV}^2$. A recent calculation [18] of the contribution of F_{mag} to $A(Q^2)$ using several n - n potentials in a variational approach indicates that above $Q^2 = 2 \text{ GeV}^2$, F_{mag} is the dominant term in $A(Q^2)$, completely altering the shape of the 2nd diffraction feature from F_{ch} . The total $A(Q^2)$ is, however, still too low by factors of 2 to 4 in the Q^2 region 0.8 to 2 GeV^2 , which remains as a serious problem.

I. Sick has made the observation [19] that the height of the second maximum in the ^3He F_{ch} is correlated with a dip in the nuclear charge density $\rho(r)$ (also in the one-body density) near the origin. A recent study [20] of the contribution of various parts of the Faddeev wave function to the charge density indicates that the height of the 2nd maximum, and therefore the size of the dip in $\rho(r)$ near $r = 0$, is directly related to the percent D state in ^3He , which in turn is related to the percent D state in the deuteron. Intuitively one can understand

ASYMPTOTIC FORM FACTORS - QUARKS IN NUCLEI

It is fairly evident now that nucleons are in some sense made of pointlike charged constituents. The general picture of hadron structure emerging from recent discoveries at e^+e^- storage rings and the growing body of deep inelastic and high transverse momentum data is one of colored quarks of various flavors bound via exchange of colored gluons into the familiar hadrons as color singlets.

There are several approaches to quark models of nuclear structure. The dimensional scaling quark model (DSQM) [16] was developed mainly in an attempt to understand the large body of high energy and large transverse momentum data. It predicts the shape of hadron electromagnetic form factors, which are a special case of the general structure functions, to be determined at asymptotic Q^2 by n , the number of constituents (quarks) in the hadron

$$A^{1/2} = F_H \sim \left(\frac{1}{Q^2}\right)^{n-1} \quad (4)$$

The power law behaviour reflects the underlying scale invariant interaction of pointlike constituents.

In Fig. 9 are plotted the world's data for the hadron form factors for $A \leq 4$ divided by the DSQM prediction. The π and proton data closely follows the predicted power law behaviour. The deuteron appears to be approaching the asymptotic shape above $Q^2 = 4 \text{ GeV}^2$, while the ^3He and ^4He data are so far known only in the preasymptotic region. These curves suggest that somewhere in the region of $Q^2 = 4$ to 6 GeV^2 the nucleon quark constituents determine the shape of the nuclear structure functions [21].

Recently Brodsky and co-workers [22] have understood the DSQM predictions for exclusive scattering processes starting from a more fundamental QCD theory of colored quarks and gluons. They are able to derive the meson and nucleon form factors, which contain the basic scale invariant terms of the DSQM plus terms containing logarithms of the QCD coupling constant that give small

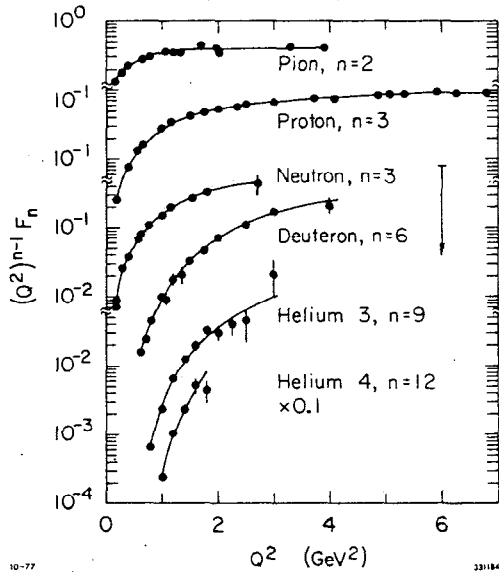


Fig. 9. Elastic electromagnetic form factors of hadrons and nuclei with $A \leq 4$ for large Q^2 , divided by the DSQM model. The curves simply connect the data points.

violations of perfect scaling at large Q^2 .

Another approach to nuclear structure in the quark model is in the context of the so-called bag models. C. DeTar has studied the [23] the interaction of six

quarks with the isotopics of the deuteron in the MIT bag model. He used the static cavity approximation and looked at the two nucleon interaction energy as the separation between the centers of mass of the neutron and proton quarks was varied. The important result is that the energy has a minimum for nucleon separations around 0.8 fm and rises at larger separation due to the color-electric force. At small separations in the region of the repulsive core, the energy rises due to the color-magnetic interaction between the quarks. DeTar has recently extended [24] this work to include the nucleon spin and he gets directly the correct sign for the tensor force and the deuteron quadropole moment from the basic quark-quark interactions. So far this simplified model is not able to produce deuteron form factors at large Q^2 . However, it is clear from this work and the QCD calculations of asymptotic form factors that the old questions about the nature of the n-n interaction inside 1 fermi are being explored from exciting new points of view, which could eventually lead to a comprehensive theory of nuclear structure starting with the quark currents.

The present form factor data for the light nuclei appear to be in the transition region between the domain of traditional nuclear physics and the quark region. Of particular interest in this transition region is the correspondence between the alternative descriptions. As a step in that direction, Carlson and Gross [4] have investigated the asymptotic shape of the structure functions in the RIA, and they find

$$\begin{aligned} A(Q) &\rightarrow Q^{-11} \\ B(Q) &\rightarrow Q^{-10} \quad \text{for } Q^2 > 4M_d^2 = 16 \text{ GeV}^2 \end{aligned}$$

This is to be compared with the DSQM prediction of $A(Q) \rightarrow Q^{-10}$. The asymptotic power of Q in the RIA can be traced to the leading terms of the expansion of the π -n interaction. If the quark model is correct, then the impulse approximation cannot dominate at large Q^2 , and perhaps as has been suggested [16], the DSQM model is an alternative description of the exchange currents which do hold up at large Q^2 .

QUESTIONS FOR FUTURE EXPERIMENTS

There are several options for future experiments in this area. More data for $A(Q^2)$ at larger Q^2 is not a likely possibility. The present limits, determined by low cross sections, are at the edge of feasibility for the present generation of accelerators, spectrometers, and targets. The ultimate limits are set by geometry (solid angles) and the tolerance of targets and detectors for high rates. There are perhaps factors of 2 to 10 to be gained with clever design and lots of money, but not two or three orders of magnitude.

Separation of the deuteron charge and quadrupole form factors G_C and G_Q would aid in untangling the knot. However, there does not now exist a technology for either polarized deuteron targets which can stand the high beam currents necessary for low cross section measurements, or a deuteron polarimeter with known analyzing

power for use at large recoil momentum.

Another possibility is to measure the magnetic structure functions at large Q^2 by doing backward angle electron scattering. Such measurements are now being proposed by our group at SLAC 25. The magnetic structure functions of the light nuclei are a rich source of information about the outstanding pieces of the puzzle. The $B(Q^2)$ functions can be isolated experimentally, and in the impulse approximation they are expected to show sharp diffractive features in the Q^2 region 0.8 to 2 GeV^2 . The exact position of the minima and the height of the second maxima are strongly related

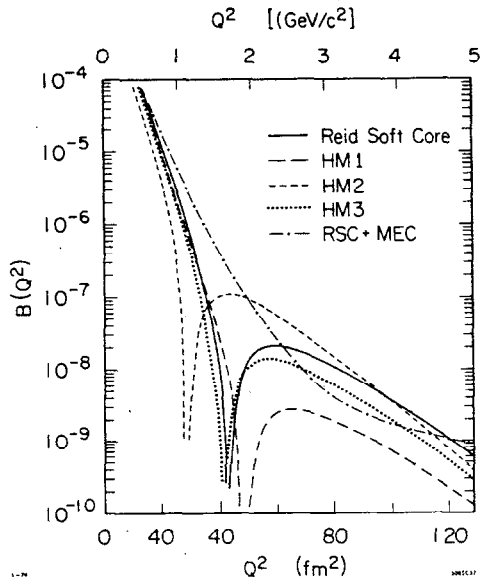


Fig. 10. The deuteron elastic structure function $B(Q^2)$ evaluated in the NRIA with dipole nucleon form factors and various 2-component deuteron models. The curves are: RSC (Ref. [8]); HM1, HM2, HM3 (Ref. [6]); RSC + MEC, Reid soft core plus meson exchange (Ref. [26]).

are available for F_{mag} in ^3He and ^3H . Barroso and Hadjimichael [28] indicate that the interference between the S and D state parts of the 3-body wave functions cause the location of the diffraction minimum in F_{mag} to shift by 6 fm^{-2} in opposite directions in ^3He and ^3H in the Q^2 region 8 to 20 fm^{-2} . The structure functions of d, ^3He and ^3H are all tightly interconnected and comparison of high Q^2 measurements in all these nuclei could place severe constraints on the models, and could perhaps give a clue to the source of the current problems in the $A(Q^2)$ functions.

POSSIBLE FUTURE EXPERIMENTS

We are proposing to measure elastic and inelastic magnetic structure functions of the light nuclei in the Q^2 range 0.6 to approximately 2 GeV^2 at SLAC using 30 to

to such properties as the percent D state, the nature of the π -n coupling, and the presence of the exchange currents. In the calculation of Gari and Hyuga [26] for the deuteron, the MEC completely alter the shape of the NRIA diffractive features in $B(Q^2)$ by filling in the minimum. These predictions for large isoscalar MEC effects in the deuteron $B(Q^2)$ can be compared to the similar effect of the isovector MEC on the diffractive features of the electrodisintegration cross section at threshold in the same Q^2 range. In practice any measurement of $B(Q^2)$ will be accompanied almost for free by a measurement of $d\sigma/d\Omega dE$ at the threshold, which would make possible a direct comparison of these features to place strong constraints on possible MEC currents.

Some of the nonrelativistic predictions for the deuteron $B(Q^2)$ are shown in Fig. 10. The present measurements [2] extend only out to $Q^2 = 25 \text{ fm}^{-2}$. Several predictions [18,27]

40 cm long targets and the Rosenbluth method at angles from 35° to 155° . The cross sections are expected to fall to the level of 10^{-36} to 10^{-40} cm^2/sr in that Q^2 range, and it is absolutely necessary to have high beam intensities in the energy range 0.5 to approximately 2 GeV and to use thick targets to achieve appreciable counting rates. Presently there does not exist such a high energy, high intensity electron beam anywhere. Beams of the required energy range are available at SLAC, but the intensity is considerably reduced by beam break up from the maximum intensity attainable with high energy beams.

To provide the incident electrons we are proposing to build an off-axis gun and in-line injector at Sector 26 of the 30 Sector linac. The new beam would be produced in the last 5 sectors of the present accelerator, could have a maximum (unloaded) energy of 3.5 GeV and have a maximum duty factor of 5.7×10^{-4} at 360 pps with a 1.6 μs pulse length. At 100 mA peak current the beam loading would reduce the maximum energy to 2.9 GeV. The beam quality would be similar to that of the present 20 GeV beams, i.e., 80% transmission through $\pm 0.2\%$ momentum slits. By installing the new injector near the output end of the linac, it will be possible to deliver beams with intensity increased 10 to 50 times over what is presently available at SLAC in that energy range due to the shortened length of accelerator contributing to beam breakup.

The new injector could be switched on and off on a pulse to pulse basis and would not interfere with high energy beams originating from the primary injector. The design is a simplified replica of the existing injector, and the total cost in FY 1980 dollars, including overhead factors, is \$0.9M. This project was recently recommended by the Nuclear Science Advisory Committee in its recommendations to DOE/NSF for the FY 1981 budget. Presently discussions are underway with DOE/NSF and the SLAC management over how this project might be carried out amid the hectic schedules for PEP construction and the usual tight funding.

The new beam will fill an energy gap in high intensity, low duty factor electron beams for nuclear structure physics between the range of the Bates-Saclay-IKO machines and the present SLAC beams. The low duty factor limits the use of the new beam to single arm inclusive reactions or to highly correlated (elastic) coincidence measurements. We are also considering for possible future proposals to add a radio-frequency energy compression system that could compress the momentum spectrum of the beam to a spread of .01% dp/p . For the present we propose to do elastic scattering in coincidence using two large SLAC spectrometers, and also to do a longitudinal-transverse separation in the quasielastic region in single arm measurements.

CONCLUSIONS

Data on electromagnetic form factors of light nuclei at large Q^2 are uniquely available from experiments using high intensity, high energy electron beams, and they can be readily produced using the present generation of low duty factor accelerator.

High Q^2 measurements probe the nuclear systems in the region of overlap between nuclear and quark physics, and such data will compliment the new results at lower Q^2 soon to come from more complicated coincidence experiments using the next generation of lower energy, but higher duty factor, accelerators being discussed at this conference.

REFERENCES

- [1] The present and past members of and collaborators with the American University Group at SLAC are: R. Arnold, B. Chertok, E. Dally, D. Day, A. Grigorian, C. Jordan, F. Martin, J. McCarthy, B. Mecking, S. Rock, I. Schmidt, W. Schütz, I. Sick, Z. Szalata, G. Tamas, R. York, and R. Zdarko.
- [2] R. Arnold et al., Phys. Rev. Lett. 35, 776 (1975), F. Martin et al., Phys. Rev. Lett. 38, 1320 (1977).
- [3] F. Gross, Phys. Rev. D10, 223 (1974) and references therein.
- [4] R. Arnold, C. Carlson, F. Gross, to be submitted for publication.
- [5] W. Buck, F. Gross, Phys. Lett. 63B, 286 (1976), and William and Mary Preprint 78-9, submitted for publication.
- [6] K. Holinde, R. Machleidt, Nucl. Phys. A256, 479 (1976), Nucl. Phys. A256, 497 (1976).
- [7] E. Loman, H. Feshbach, Ans. Phys. (NY) 48, 94 (1968).
- [8] R. Reid, Ans. Phys. (NY) 50, 411 (1968).
- [9] F. Iachello, A. Jackson, A. Lande, Phys. Lett. 43B, 191 (1973).
- [10] S. Galster et al., Nucl. Phys. B32, 221 (1971).
- [11] R. Arnold et al., Phys. Rev. Lett. 40, 1429 (1978).
- [12] J. S. McCarthy et al., Phys. Rev. C15, 1396 (1977) and references therein.
- [13] R. Brandenburg et al., Phys. Rev. C12, 1368 (1975).
- [14] A. Laverne, C. Gignoux, Phys. Rev. Lett. 29, 436 (1972).
- [15] J. Borysowicz, D. Riska, Nucl. Phys. A254, 301 (1975).
- [16] The DSQM model is the work of many people. For an investigation of the hadron form factors, see S. Brodsky, B. Chertok, Phys. Rev. D14, 3003 (1976) and references therein.
- [17] I. Schmidt, R. Blankenbecler, Phys. Rev. D15, 3321 (1977), Phys. Rev. D16, 1318 (1977).
- [18] T. Katayama, Y. Akaishi, H. Tanaka, Hokkaido University Preprint HOUP-78118, Japan (1978).
- [19] I. Sick, Proceedings of Workshop on Few Body Systems and Electromagnetic Interactions, Frascati, 1978.
- [20] P. Groenenboom, H. Boersma, Universiteit Amsterdam, Preprint (1978).
- [21] See also B. Chertok, Phys. Rev. Lett. 41, 1155 (1978) for a study of the ^3He and ^4He form factors in the preasymptotic Q^2 region using modified versions of the DSQM.
- [22] S. Brodsky, G. Lepage, SLAC-PUB-2294 and references therein.
- [23] C. DeTar, Phys. Rev. D17, 302 (1978), and D17, 323 (1978).
- [24] C. DeTar, University of Utah Preprint UU HEP 78/1 (1978).
- [25] R. Arnold et al., Proposal for Measurement of Electron-Deuteron Elastic and Inelastic Magnetic Structure Functions at Large Momentum Transfer, SLAC Experiment E134 (1978).
- [26] M. Gari, G. Hyuga, Nucl. Phys. A264, 409 (1976), and Nucl. Phys. A278, 372 (1977).
- [27] M. Haftel, W. Kloet, Phys. Rev. C15, 404 (1977) and references therein.
- [28] A. Barroso, E. Hadjimichael, Nucl. Phys. A238, 422 (1975).